Accepted Manuscript

Research Paper

Nanoparticles decorated with proteolytic enzymes, a promising strategy to overcome the mucus barrier

Irene Pereira de Sousa, Beatrice Cattoz, Matthew D. Wilcox, Peter C. Griffiths, Robert Dagliesh, Sarah Rogers, Andreas Bernkop-Schnürch

Please cite this article as: I. Pereira de Sousa, B. Cattoz, M.D. Wilcox, P.C. Griffiths, R. Dagliesh, S. Rogers, A. Bernkop-Schnürch, Nanoparticles decorated with proteolytic enzymes, a promising strategy to overcome the mucus barrier, *European Journal of Pharmaceutics and Biopharmaceutics* (2015), doi: http://dx.doi.org/10.1016/j.ejpb. 2015.01.008

Nanoparticles decorated with proteolytic enzymes, a promising strategy to overcome the mucus barrier

Pereira de Sousa, Irene [1]; Cattoz, Beatrice [2]; Wilcox, Matthew D.[3]; Griffiths, Peter C.[2]; Dagliesh, Robert[4]; Rogers, Sarah[4] and Bernkop-Schnürch, Andreas [1*]

[1]*Department of Pharmaceutical Technology, Institute of Pharmacy, Leopold-Franzens-University of Innsbruck, Innrain 80/82, 6020 Innsbruck, Austria*

[2]*Department of Pharmaceutical, Chemical and Environmental Sciences, Faculty of Engineering and Science, University of Greenwich, Medway Campus, Central Avenue, Chatham Maritime, Kent, ME4 4TB, U.K.*

[3]*Newcastle University, Institute for Cell and Molecular Biosciences, Framlington Place, Newcastle upon Tyne, NE2 4HH, United Kingdom*

[4]*ISIS Facility, Science and Technology Facilities Council, Rutherford Appleton Laboratory, Harwell Science and Innovation Campus, Didcot OX11 0QX, UK*

*Corresponding author: Andreas Bernkop-Schnürch

Department of Pharmaceutical Technology, Institute of Pharmacy, University of Innsbruck

Center for Molecular Biosciences (CMBI)

Innrain 80/82, 6020 Innsbruck, Austria

e-mail: andreas.bernkop@uibk.ac.at

Tel.: +43 512 507 58600

Fax: +43 512 507 58699

1. ABSTRACT

The intestinal mucus gel layer represents a stumbling block for drug adsorption. This study is aimed to formulate a nanoparticulate system able to overcome this barrier by cleaving locally the glycoprotein substructures of the mucus. Mucolytic enzymes such as papain (PAP) and bromelain (BRO) were covalently conjugated to poly(acrylic acid) (PAA). Nanoparticles (NPs) were then formulated via ionic gelation method and characterized by particle size, zeta potential, enzyme content and enzymatic activity. The NPs permeation quantified by rotating tube studies was correlated with changes in the mucus gel layer structure determined by pulsed-gradient-spin-echo NMR (PGSE-NMR), small-angle neutron scattering (SANS) and spin-echo SANS (SESANS). PAP and BRO functionalized NPs had an average size in the range of 250 and 285 nm and a zeta potential that ranged between -6 and -5 mV. The enzyme content was 242 µg enzyme/mg for PAP modified NPs and 253 µg enzyme/mg for BRO modified NPs. The maintained enzymatic activity was 43% for PAP decorated NPs and 76% for BRO decorated NPs. The rotating tube technique revealed a better performance of BRO decorated NPs compared to PAA decorated NPs, with a 4.8 fold higher concentration of NPs in the inner slice of mucus. Addition of 0.5wt% of enzyme functionalized NPs to 5wt% intestinal mucin led to c.a. 2 fold increase in the mobility of the mucin as measured by PGSE-NMR indicative of a significant break-up of the structure of the mucin. SANS and SESANS measurements further revealed a change in structure of the intestinal mucus induced by the incorporation of the functionalized NPs mostly occurring at a lengthscale longer than 0.5 µm. Accordingly, BRO decorated NPs show higher potential then PAP functionalized NPs as mucus permeating drug delivery systems.

Keywords: mucus permeating nanoparticles, papain, bromelain, oral drug delivery

2. INTRODUCTION

Among all the administration routes the oral one is the most favorable, however the low oral bioavailability of numerous drugs is a major issue and strategies able to improve drug solubility and adsorption are needed. One of the main causes of low drug oral bioavailability is the presence of a barrier that covers all the surface of the GI tract, namely the mucus barrier. This continuous gel layer is a complex matrix formed mainly by mucin, a polypeptide with highly glycosylated negatively charged regions, hydrophobic regions and cysteine rich regions interconnected via disulfide bonds. Mucus is a semipermeable barrier that guaranties the exchange of nutrients, gases and water and prevents the permeation of many pathogens and foreign particles [1]. In recent years many attempts have been undertaken to formulate drug delivery systems (DDSs) able to overcome this barrier. A strategy that showed potential was a nanoparticulate system bearing mucolytic agents able to cleave the mucus substructure in front of them and therefore to cross this barrier. An *in vivo* study showed a prolonged residence time, compared to not functionalized NPs, in the small intestine of rats [2]. As this preliminary study showed great potential, it is worth to continue working in this direction to further improve such systems and the analytical methods needed behind. Accordingly, it was the aim of this study to compare the features of the papain (PAP) conjugated nanoparticles (NPs) with a new carrier bearing bromelain (BRO). **The chosen enzymes are stable in simulated intestinal fluid as demonstrated by in vitro studies and their maintained mucolytic activity and ability to permeate through the intestine was demonstrated by several in vivo studies [3-6]. However the enzymes are digested in gastric environment and therefore enteric coat is necessary for in vivo application.** Both enzymes are known to decrease the intestinal mucus viscosity [7] but, to our knowledge, a systematic comparison between PAP and BRO modified NPs has not been performed yet. BRO was selected for the formulation of functionalized NPs in order to improve the tolerability of the carrier. In fact, beside the known occupational allergy caused by both enzymes **(means a long term work**

3

related exposure) [8-11], just one case of allergic reaction associated with BRO ingestion could be found in the literature [12], while several cases of non-occupational allergic sensitization were reported for PAP [13, 14]. Moreover, a series of clinical trials were performed in the past decade, last one published in 2013, illustrating the good tolerability to BRO ingestion by patients [15-18]. Poly(acrylic) acid was chosen as polymeric backbone for this DDS as it shows weak mucoadhesive properties [19] and bears carboxylic groups to which enzymes can be conjugated via carbodiimide chemistry [20]. The reaction can take place at the amino terminal group of both enzymes and at lysine residues, which are 10 for PAP and 15 for BRO [21, 22]. To further investigate and gain a deeper understanding of the enhancing permeation properties of this new DDS, the results obtained with previously established techniques were correlated with the results obtained exploiting innovative techniques (such as pulsed-gradient spin-echo NMR, small-angle neutron scattering and spin-echo small angle neutron scattering) yielding information on the effect of these NPs on the structure of mucus at small lengthcales.

3. MATERIALS AND METHODS

3.1. Materials

Poly(acrylic) acid (PAA, **solution 35wt% in H$_2$O, average molecular weight 100 kDa**), papain from carica papaia 3.6 U/mg (EC 3.4.22.2), bromelain from pineapple steam 3.4 U/mg (EC 3.4.22.32), 1-Ethyl-3-(3-dimethylaminopropyl)carbodiimide (EDAC), N-hydroxysuccinimde (NHS), ethylenediaminetetraacetic acid (EDTA), casein, L-cysteine, trehalose, trichloroacetic acid (TCA), resazurin and all other salts and solvents at analytical grade were purchased from Sigma – Aldrich (Vienna, Austria). Lumogen red was purchased from Kremer pigmente GmbH & Co. KG (Aichstetten, Germany). Bicinchoninic acid kit (BCA) was purchased from Thermo Scientific (Vienna, Austria). Minimum essential medium (MEM) was purchased from Biochrome AG (Berlin, Germany). Intestinal mucin (Imucin) and intestinal mucus (Imucus) were obtained from Jeff Pearson (Newcastle University, Institute for Cell and Molecular Biosciences, Newcastle upon Tyne, United Kingdom).

3.2. Polymer synthesis

3.26 g of PAA solution, corresponding to 1 g of polymer (MW 100 kDa, 0.01 mmol), was diluted in 1 L of water, pH adjusted to 6, to obtain a 0.1wt% solution. 5 g of EDAC (191.7 Da, 26.08 mmol) and 3 g of NHS (115.09 Da, 26.07 mmol) were dissolved in 100 mL of water and added to the polymer solution. The reaction mixture was incubated for 1 h under vigorous stirring. Then, 1 g of PAP (theoretical molecular weight 23.4 kDa, 0.043 mmol [23]) or 1.42 g of BRO (approximate molecular weight 33 kDa, 0.043 mmol [24]) was dissolved in 500 mL of water and slowly added to the reaction mixture and stirred for 24 h at 10°C. The obtained enzyme-polymer conjugate was dialyzed against demineralized water for 3 days at 10°C. The solutions were then lyophilized yielding a white powder referred as PAA-PAP and PAA-BRO, respectively [2].

3.3. Nanoparticles formulation

100 mg of PAA or enzyme-polymer conjugate were dissolved in 10 mL water to obtain a 1wt% solution and the pH was adjusted to 8. This mixture was slowly added to 7.5 mL of Lumogen aceton solution 0.07 mg/mL. After 10 min equilibration 1 mL of $CaCl_2$ 5 mg/mL dissolved in water was added drop by drop and stirred for 30 min. The suspension was then centrifuged at 5500 rpm (4966 x g) for 25 min (MiniSpin centrifuge, Eppendorf), the supernatant discarded and the pellet washed with 50vol% aceton/water mixture for three times. Finally the washed pellet was resuspended in 1wt% trehalose/water solution by means of probe sonication for 10 sec and then lyophilized. The obtained products were referred to PAA NPs when PAA was used for the formulation, PAA-PAP NPs when PAA-PAP was used for the formulation and PAA-BRO NPs when PAA-BRO was used for the formulation.

3.4. Nanoparticles characterization

Nanoparticle particle size and charge characterization was carried out by using a NICOMPTM 380 ZLS PSS (Particle Sizing Systems, CA, USA). Particle size was recorded at a scattering angle of 90° for 10 min at room temperature. Zeta potential was recorded under electric field strength of 5 V/cm for 3 minutes at room temperature.

3.5. Enzyme quantification

The amount of enzyme conjugated to polymers and nanoparticles was determined by micro BCA protein assay, following the provider´s instruction. The samples were dissolved in 0.1 M NaOH solution containing 1.5wt% of sodium dodecyl sulfate to obtain a concentration of 0.1 mg/mL. The samples were incubated at 25°C in a thermomixer (Thermomixer Conform; Eppendorf, Hamburg, Germany) under constant shaking, 1000 rpm for 2 h. Thereafter, 150 µL of sample were mixed with 150 µL of working reagent in a 96 well plate and incubated for

further 2 h at 37°C. Finally the absorbance was detected at 562 nm by using a microplate reader (TECAN Infinite M200, Austria GmbH). The amount of enzyme was extrapolated by fitting the data to a calibration curve obtained via analyzing solution with different concentration of PAP or BRO. The enzyme content of polymers and NPs was reported on a weighted base as the ratio between the amount of conjugated enzyme and the amount of polymers or NPs. The conjugation efficacy onto the polymers was calculated as weight percent of the amount of conjugated enzyme relative to the initial amount of enzyme used.

3.6. Enzymatic activity assay

The remaining enzymatic activity of conjugated enzyme was detected via casein assay [25]. **The polymers** were dissolved **and the particles were dispersed** at a concentration between 0.5 and 1 mg/mL in PBS 50 mM pH 8 containing 2 mM EDTA and 5 mM L-cysteine. The solutions were then diluted with 2 mL of PBS 10 mM pH 8 and further with 1 mL of 2wt% casein solution. The reaction mixtures were incubated for 30 min at 37°C in a thermomixer under constant shaking, 750 rpm. After incubation 120 µL of 100wt% TCA solution was added in order to stop the reaction. The samples were then centrifuged for 10 min at 13400 rpm (12100 x g) and the absorbance of the supernatant detected at 280 nm. The assay was performed in parallel with solutions presenting the same enzyme concentration of each sample. The remaining enzymatic activity of the enzyme-conjugated samples was calculated as percentage comparing the absorbance of the samples and the pure enzyme solutions.

3.7. **Cytotoxicity** assay

The cytotoxicity of polymers and NPs was tested in Caco-2 cells by resazurin assay. Caco-2 cell were seeded on 96-well plates at a concentration of 10^4 cells/well and cultivated for 24 h at 37°C and 5% CO_2. Thereafter, the medium was discarded and 100 µL of polymers and NPs

7

dissolved/**dispersed** in MEM **not supplemented with fetal bovine serum** at different concentration (0.1-2 mg/mL) was added. After 4 h incubation to each well 100 µL of resazurin solution 88 µM dissolved in not supplemented MEM was added and incubated for 2 h. Finally the fluorescence intensity (λ_{ex} 540 nm, λ_{em} 590 nm) was determined. **As control, 100 µL of polymers and NPs dissolved/suspended in not supplemented MEM at different concentrations (0.1-2 mg/mL) were incubated without cells for 4 h. Theses samples were treated with resazurin as described above and the fluorescence intensity was measured. The fluorescence intensity of the samples incubated without cells was subtracted to the fluorescence intensity of the samples incubated with cells at the same concentration.** The data were reported as percentage of viable cells considering the **negative** control (cells incubated with MEM) as 100% viability. **As positive control Triton X 1wt% dissolved in MEM was used.**

3.8. Intestinal mucus collection

Pig small intestines were obtained from a local abattoir immediately after slaughter and transported on ice to the laboratory. Sections of the intestines that did not visibly contain chyme were cut into ~15 cm lengths and mucus was removed. To remove the mucus gentle pressure was applied to one end of the length with the fingers and continuously applied unidirectionally to the opposite end. If the mucus contains debris the mucus was cleaned as follows. The mucus was gently stirred (<100 rpm) for 1 h at 4°C in sodium chloride (0.1 M) at a ratio of 1 g mucus to 5 ml sodium chloride. The mixture was then centrifuged at 9000 rpm (10,400 x g) at 10°C for 2 h. The supernatant was discarded as well as the granular material at the bottom. The clean portion of the mucus was added to half the volume of sodium chloride (0.1 M) used for first washing. This was stirred (<100 rpm) for 1 h at 4°C and then centrifuge at 9000 rpm at 10°C for 2 h. The supernatant was discarded and only the

8

clean portion of the mucus was collected. Cleaned mucus (Imucus) was stored in aliquots at -20°C until use.

3.9. Mucin purification from porcine mucus

Mucus gel was collected as described above but added to a cocktail of enzyme inhibitors in phosphate buffer, pH 6.8 [26]. The mucus was not cleaned prior to mucin purification. The mucin (Imucin) was purified following the protocol described by Taylor et al., with the addition of a second caesium chloride gradient to further remove cellular debris from the glycoprotein component of mucus. All freeze dried sample were stored at -20oC until used.

3.10. Permeation study

The permeation ability of the prepared NPs was investigated by the rotating tube technique [27]. Plastic tube with a length of 30 mm and a diameter of 4 mm were filled in with Imucus exploiting a syringe without needle. One end of the tube was closed with parafilm, on the other end 100 µL of NPs, (previously resuspended by means of probe sonication for 10 sec in simulated intestinal fluid without pancreatin (SIF) (1 mg/mL)), was added. For each sample six replicates were prepared. After preparation the tubes were incubated at 37°C for 4 h under a constant horizontal stirring (≈50 rpm). **A scheme representing the system is illustrated in Figure 1**. Thereafter, the tubes were frozen at -80°C and cut into slices of 2 mm length. Each slice was incubated with 150 µL DMSO, left overnight at room temperature protected from light and then ultrasonicated for 1 h. After centrifugation for 2 min at 13400 rpm (12100 x g) the fluorescence intensity of the supernatant (λex 578 nm, λem 613 nm) was determined in order to assess the depth of particles diffusion into the mucus. As control, the test was run each time with a tube filled with Imucus without NPs. The obtained fluorescence intensity of the Imucus was subtracted to the fluorescence intensity of the samples.

9
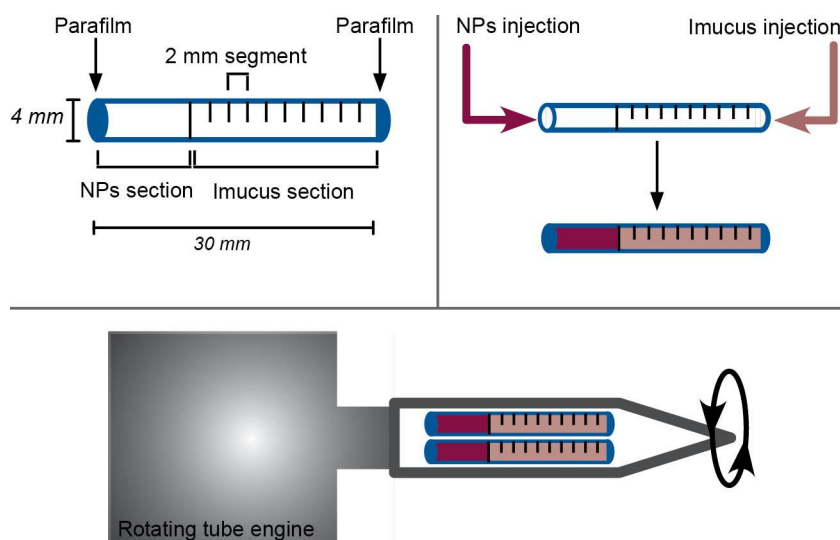
Figure 1. Schematic representation of the rotating tube technique.

3.11. Pulsed-gradient spin-echo NMR assessment of mucin mobility

Pulsed-gradient spin-echo NMR (PGSE-NMR) measurements were performed on a Bruker DMX400 NMR spectrometer operating at 400 MHz (^{1}H) using a stimulated echo sequence [28]. All the experiments were run at 37ºC using the standard heating/cooling system of the spectrometer to an accuracy of ±0.3ºC. All solutions were prepared from stock solutions and made up in SIF with the exception that D_2O was used in place of H_2O. The NPs formulations (containing calcium chloride and trehalose) were dispersed in SIF to a concentration of 0.5wt% NPs (equivalent to 7.5wt% of formulation). Imucin was then dissolved in the respective samples **(final concentration 5wt%)** and left to equilibrate for 24h. 0.6 mL were transferred to 5 mm o.d. NMR tubes (Willmad NMR tubes form Sigma-Aldrich).

Generally, the self-diffusion coefficient, D, is deduced by fitting the attenuation (decay) of the integral for a chosen peak to eqn.1,

$$A(\delta, G, \Delta) = A_0 \exp(-kD) \tag{1}$$

where A is the signal intensity and $k = -\gamma^2 G^2 \delta^2 (\Delta - \delta/3)$, where γ is the magnetogyric ration, Δ

10

the diffusion time, δ the gradient pulse length, and G is the gradient field strength. The gradient pulses are ramped to their desired value over a ramp time, σ, typically 250 µs.

For complex spectra such as those encountered here, the diffusion data are better analysed by fitting to this equation the entire bandshape using "CORE", a program devised to resolve the various components present in such data [29]. CORE permits the selection of significant regions of peak intensity within the spectra as well as the ability to "mask out" any unwanted regions **, such as peak e.g. H_2O arising from background components of no interest**. CORE evaluates the experimental data in two dimensions by a global least squares fit, yielding estimations of the diffusion coefficients for each component in the sample. The output data include the fitted parameters of the optimized model, the global fit and the global difference map.

3.12. SANS and SESANS

Small-angle neutron scattering (SANS) is a powerful technique for determining microstructure in the dimension range of 1 to 400nm. SANS experiments were performed on the fixed-geometry, time-of flight SANS2D diffractometer at the ISIS Spallation Neutron Source, Rutherford Appleton Laboratory (Didcot, United Kingdom). A $Q = (4\pi/\lambda) \sin(\theta/2)$ range between 0.004 and 0.3 $Å^{-1}$ is obtained by using neutron wavelengths (λ) spanning 1.8 to 16.5 Å with a fixed sample-detector distance of 4.0 m. The samples were contained in demountable 1 mm path length, UV-spectrophotometer grade, quartz cuvettes (Starna) and mounted in aluminum holders on top of an enclosed, computer-controlled, sample chamber. All experiments were conducted at 37 °C. NPs and free enzymes were incubated with Imucus for 3 hours prior to measurement. The concentration of free enzyme in the samples was chosen to be equivalent to the amount of enzyme present in the samples containing enzyme conjugated NPs. All scattering data were (a) normalized for the sample transmission, (b)

background corrected using a quartz cell filled with D_2O, and (c) corrected for the linearity and efficiency of the detector response using the instrument specific software package.

Spin-echo small angle neutron scattering (SESANS) is a newer technique allowing the determination of material structure in the length range between 300 and 6000 nm. In this experiment, the neutron beam was split and the two halves polarized. Since polarized and non-polarized neutrons probe structure differently, the ratio of their intensities becomes a measure of any structure present, over a distance scale defined by the evolution period used in the experiment. The latter allows us to extend the lengthscale probed by several orders of magnitude. In both experiments, the effect of free enzymes or enzyme conjugated NPs on the sample scattering was followed for a period of c.a. 5h.

3.13. Statistical data analysis

All experiments were performed with at least three replicates and the data are reported as mean ± standard deviation (SD). Statistical data analyses were performed by Student´s t-test, calculated with GraphPad Prism version 5.01. The utilized minimum level of significance was $p < 0.05$.

4. RESULTS

4.1. Polymer synthesis

PAP and BRO were successfully conjugated to the PAA backbone. The reaction was repeated four times for each enzyme showing reproducibility, the results are reported as mean of the different experiments. The synthesis procedure resulted to be efficient with a product recovery of about 59-73% depending on the enzyme used. For the reaction an equal amount of PAP and BRO expressed in mmol, calculated **making use** of the enzyme theoretical molecular weight was **exploited** in order to obtain the most similar degree of enzyme conjugation to the PAA backbone. The conjugation efficacy, calculated as described above, was slightly higher for PAA-BRO than for PAA-PAP. This resulted in greater enzyme content on a weighted base for PAA-BRO compared to PAA-PAP as reported in **Table 1**. The enzyme conjugation onto the polymeric scaffold provoked a loss of enzyme activity, when compared to the native enzyme activity, of about 58% and 37% for PAP and BRO, respectively. **In order to detect the maximum enzymatic activity the assay was performed in presence of cysteine, a common activator of cysteine proteases, such as papain and bromelain, exhibiting a nucleophilic cysteine thiol in their catalytic triad.**

Table 1. Characteristics of the **enzyme-polymer conjugates**. Results are the mean of four different synthesis of each polymer ($\pm$ standard deviation).

Polymer	Yield %	Enzyme content µg/mg	Enzyme content nmol/mg	Enzyme conjugation efficacy %	Enzymatic activity %
PAA-PAP	72.59 ± 23.60	230.09 ± 71.32	9.83 ± 3.05	30.01 ± 8.39	42.21 ± 19.54
PAA-BRO	59.16 ± 15.19	338.40 ± 78.48	10.24 ± 2.38	44.67 ± 14.43	63.31 ± 20.72

4.2. Nanoparticles formulation and characterization

NPs were formulated by ionic gelation method exploiting Ca^{2+} as counter ion. The NPs formation was optimal at pH 8 as the polymers were sufficiently charged to interact with Ca^{2+} ions. The characteristics of the NPs resuspended in SIF after lyophilization as mean of four different **preparation per formulation** are reported in **Table 2**. Enzyme-conjugated and unmodified NPs were monodispersed with a diameter included between 235 nm and 285 nm. The zeta potential resulted to be negative for all three formulations with slightly higher values for the enzyme-modified NPs. This decrease in negative charges for the modified NPs could confirm the formation of the covalent bound between the mucolytic agent and the carboxylic group of PAA. The NPs were stable during centrifugation and lyophilization with trivial variation in size and poydispersity index (data not showed). The enzyme content for PAA-PAP NPs and PAA-BRO NPs**, assessed after treatment with 1.5wt% sodium dodecyl sulfate leading to particles disaggregation (confirmed by DLS measurement),** was comparable for both products. On the contrary, BRO maintained an higher enzymatic activity compared to the native enzyme in respect to PAP. The enzyme activity loss after NPs formation was equal to 57% and 24% for PAA-PAP NPs and PAA-BRO NPs, respectively.

Table 2. Characteristics of the tested nanoparticles. Results are the mean of four different formulations per each sample ($\pm$ standard deviation).

NPs	Particle size (nm)	Polydispersity index	Zeta potential (mV)	Enzyme content µg/mg	Enzyme content nmol/mg	Enzymatic activity %
PAA NP	234.87 ± 50.39	0.11	-9.37 ± 2.00			
PAA-PAP NP	257.07 ± 109.38	0.19	-6.35 ± 3.63	242.02 ± 120.72	10.34 ± 5.16	43.14 ± 5.39
PAA-BRO	285.27 ±	0.20	-5.09 ± 0.49	253.31 ±	7.68 ±	76.04 ±

NP	119.61	120.55	3.65	8.08

4.3. Cytotoxicity test

The cytotoxycity of polymers and NPs was tested *in vitro* via resazurin assay. Both PAP modified polymer and NPs resulted to be not toxic at all the concentrations tested. PAA-BRO was found to be more toxic compared with PAA-PAP with a cell availability of about 50% at all concentrations tested. On the contrary, BRO functionalized NPs were not significantly toxic at concentration lower then 0.2 mg/mL (**Figure 2**).
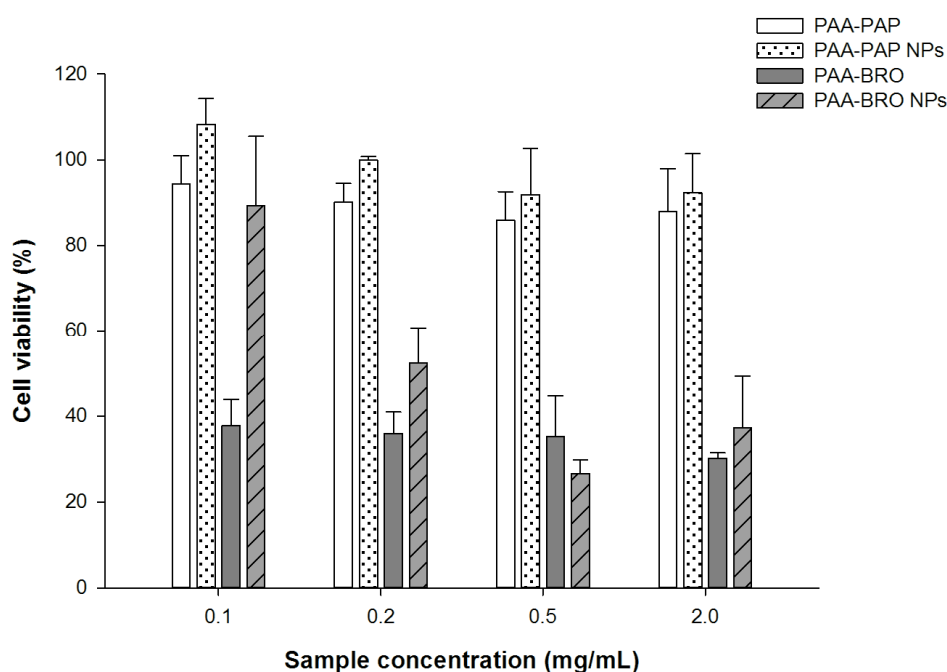

Figure 2. Cytotoxicity of PAA-PAP (white bars), PAA-PAP NPs (dotted bars), PAA-BRO (gray bars) and PAA-BRO NPs (striped bars) determined by resazurin assay after 4 h incubation with Caco-2 cells. Values are the means of three experiments (± standard deviation).

4.4. Permeation study

The permeation study assessed the depth of NPs diffusion into porcine Imucus. Both PAA-

15

PAP NPs and PAA-BRO NPs could permeate till the last Imucus segments while unmodified PAA NPs were detected only in the first few Imucus segments. These results confirm that particulate systems formulated with mucolytic enzyme conjugated polymers exhibit enhanced permeation compared to non-decorated DDS. Moreover, these results indicate higher permeation ability for PAA-BRO NPs compared with PAA-PAP NPs. In fact, at segment 3 the concentration of PAA-BRO NPs is 4.8 fold higher in respect to PAA-PAP NPs, meaning that a higher percentage of BRO decorated NPs possess the ability to permeate the Imucus barrier in comparison to the PAP-modified system (**Figure 3**).
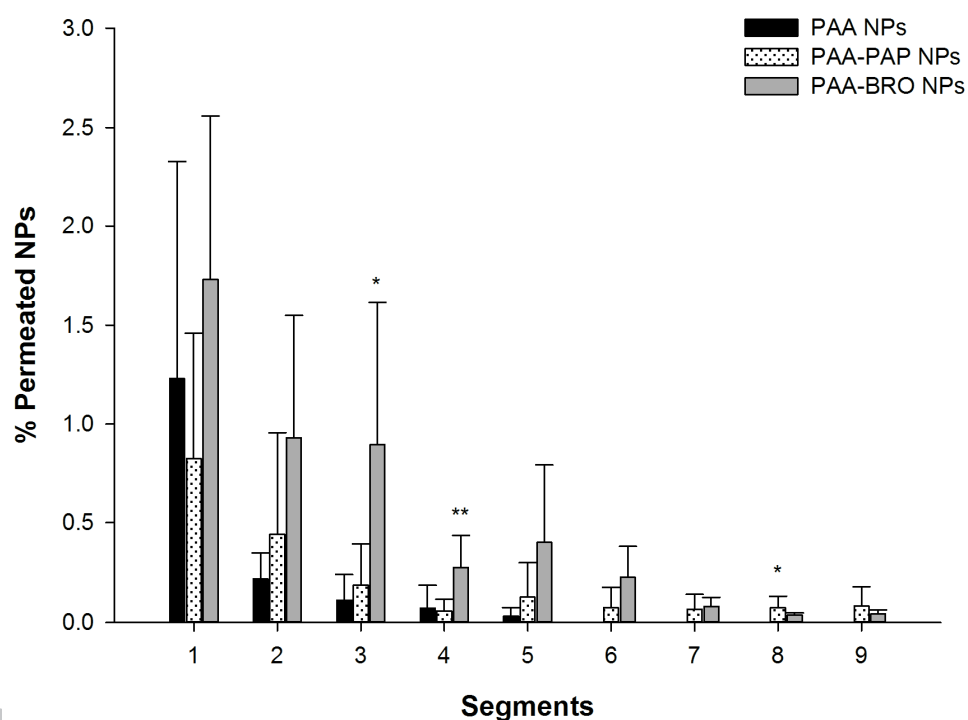
Figure 3. Permeation studies of PAA NPs (black bars), PAA-PAP NPs (dotted bars) and PAA-BRO NPs (gray bars), in porcine Imucus. Particles suspended in SIF pH 6.8 were incubated for 4 h at 37°C. * $p < 0.05$ vs PAA NPs, ** $p < 0.05$ vs PAA-PAP NPs. Values are the means of six experiments (± standard deviation).
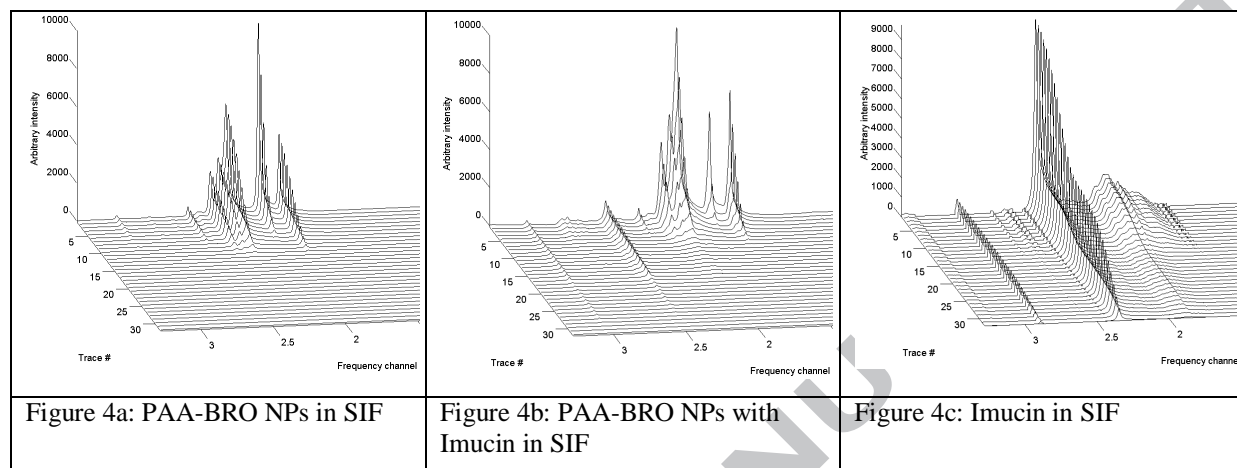
4.5. PGSE-NMR

Diffusion measurements of PAA NPs and enzyme conjugated NPs incubated in simple SIF or 5wt% Imucin in SIF were undertaken by PGSE-NMR, Figure 4. a-c. The intensity of a given peak or series of peaks in the NMR spectrum decreases as a function of increasing field gradient strength, in essence, quantifying the displacement the mucin molecules during a fixed time. A rapidly decaying signal corresponds to a high mobility, and a large diffusion coefficient.

Analysis of these diffusion data for simple NPs incubated in SIF revealed that the single in the NMR spectrum arose entirely from the stabilizer (trehalose), Figure 4.a, as anticipated, since the signal from the NPs is too weak to be visible. The analysis hence focused on changes observed in the diffusion rate of the mucin in the sample, rather than the particle itself, a rather appealing contrast to the particle diffusion in the rotating tube experiment. Since, trehalose is also visible in the samples incubated with Imucin, the diffusion coefficient attributed to trehalose was then ignored and only the signal corresponding to the mucin was considered in the analysis. These diffusion coefficients, as well as the diffusion coefficient ratio of the diffusion of Imucin alone and the diffusion coefficient of the Imucin when incubated with NPs are reported in Table 3.

As may be seen, the diffusion coefficient of mucin is only weakly affected by the blank PAA NPs confirming the absence of any significant attractive interactions between the PAA and the mucin gel. On the other hand, enzyme conjugated NPs lead to a 2 fold increase in Imucin diffusivity, indicating that the Imucin is more mobile due to the destruction of its structure. Precisely, Imucin showed a greater diffusion coefficient ration when incubated with PAA-BRO NPs (2.4) compared to PAA-PAP NPs (1.9). It is also worth noting that the sample containing Imucin alone fitted best to **two** diffusion coefficients ($D_{fast}=4.2*10^{-11}m^2.s^{-1}$ (75% of signal), $D_{slow}=1.3*10^{-13}m^2.s^{-1}$ (25% of signal) highlighting the heterogeneous nature of the sample, *i.e.* gelled and non-gelled components. The sample containing Imucin incubated with blank PAA NPs also fitted best to 2 diffusion coefficients (similar values to I mucin only); the

samples incubated with enzyme conjugated NPs, however, fitted best to 1 diffusion coefficient indicating that the stiff gel part of the Imucin no longer exists, an insight that would not be accessible by any other technique.

| Figure 4a: PAA-BRO NPs in SIF | Figure 4b: PAA-BRO NPs with Imucin in SIF | Figure 4c: Imucin in SIF |

Figure 4. Raw PGSE-NMR data from which the diffusion coefficient of the Imucin and related components were extracted.

Table 3. Absolute and relative diffusion coefficients for Imucin in the presence of the three nanoparticles; PAA NPs, PAA-PAP NPs and PAA-BRO NPs.

|	Diff coef /10^{11} $m^2.s^{-1}$	Diffusion coefficient ratio (Diff $_{sample}$/Diff$_{mucin}$)
Imucin only	3.2	1
With PAA NPs	2.8	0.9
With PAA-PAP NPs	6.0	1.9
With PAA-BRO NPs	7.6	2.4

4.6. SANS and SESANS

Two rather different neutron experiments were employed to characterise the structure of mucus over quite wide ranges of length-scale to map the molecular level interactions to the macroscopic scale. **The effect on the mucus scattering of the presence of (i) enzyme alone, and (ii) enzyme conjugated particles has been explored. Figures 5 and 6 show the SANS**

18

from (i) Imucus alone, (ii) Imucus incubated with 1wt% enzyme conjugated NPs and (iii) Imucus incubated with an equivalent amount of free enzyme. Figure 5 refers to the PAP case, figure 6 the BRO. The scattering from Imucus exhibits a strong $Q^{-2.6}$ dependency characteristic of the fractal-like structure of a dense gel network [30, 31]. The samples incubated with particles or enzymes show essentially identical scattering, as the mucus is the main component. No scattering arising from the NPs or the enzymes is expected. The lack of change in the Imucus scattering indicates that the structure of mucus is not significantly affected by either free enzyme or enzyme conjugated NPs, at least on the lengthscale probed here, i.e. 1-400 nm. Subtle changes were observed in the scattering - slight inflection at $Q=0.1\text{Å}^{-1}$ – in those samples containing PAA-PAP and PAA-BRO NPs indicative of a structure with a dimension/spacing of around 6.5 nm.
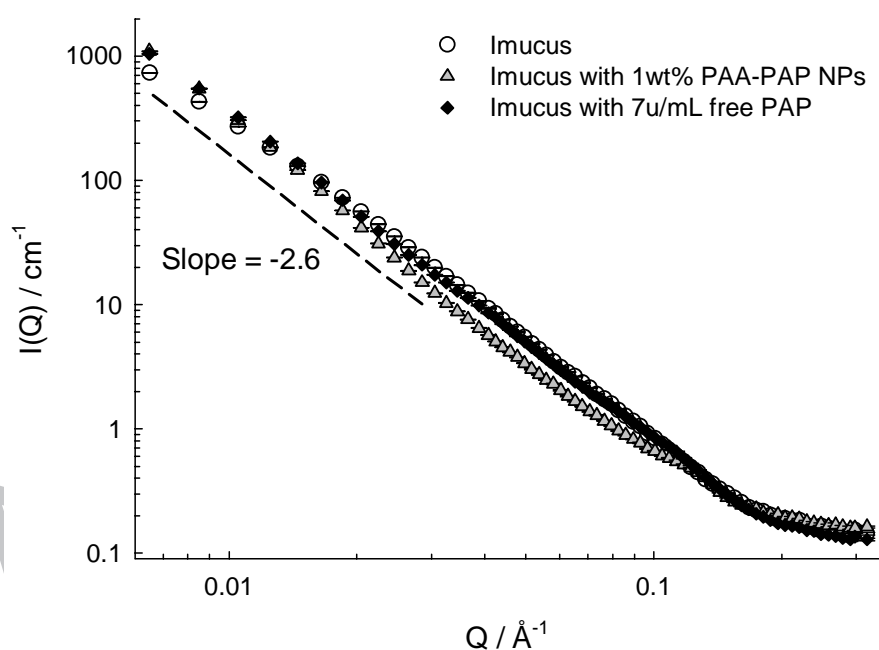
Figure 5. Scattering intensity I(Q) as a function of wavevector Q for Imucus and the same in the presence of 1wt% PAA-PAP NPs and the equivalent amount of free enzyme.
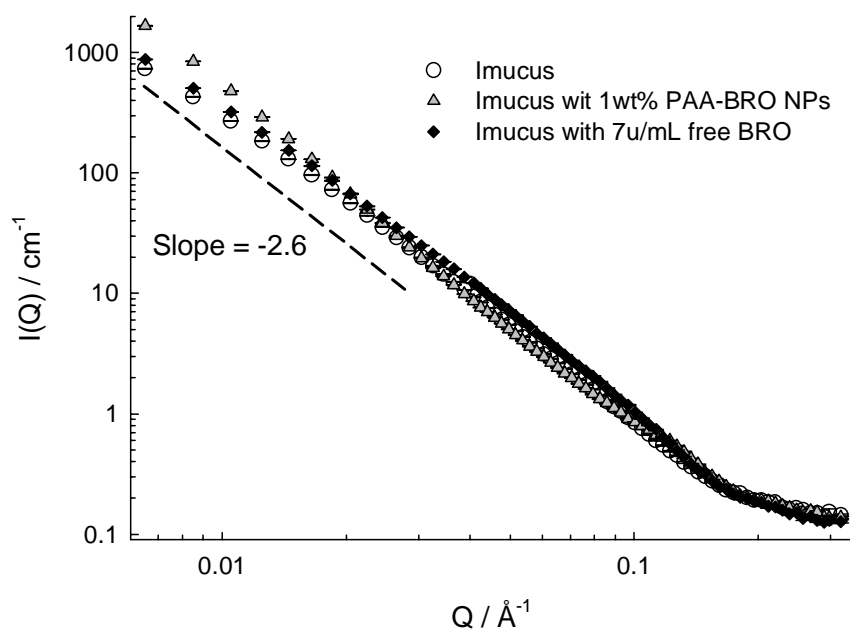
Figure 6. Scattering intensity I(Q) as a function of wavevector Q for Imucus and the same in the presence of 1wt% PAA-BRO NPs and the equivalent amount of free enzyme.

Particle-induced changes in the mucus gel structure were observed on the larger length-scales – *i.e.* the SESANS data rather than the SANS data as shown in Figures 7 and 8. A similar maximum correlation length of *c.a.* 3.50μm (that can be read off the Spin echo length axis for each curve where the depolarisation $ln\left(\frac{P_{sample}}{P_0*\lambda}\right)$ does not decrease anymore) is observed in the mucus samples before and after incubation with NPs indicating that this the gel is not affected up to this lengthscale. The larger depolarisation (decrease in $ln\left(\frac{P_{sample}}{P_0*\lambda}\right)$) for the mucus samples incubated with NPs indicates that a structural change has occurred and the samples appear more compact which may be imputed to a local breaking down of the gel network.

These two scattering techniques taken together imply that the local structure of the gel defined by the component polymers is retained (and hence for example the stiffness of the gel), but

that the larger lengthscale changes are manifest *via* a perturbation in the cross-link density
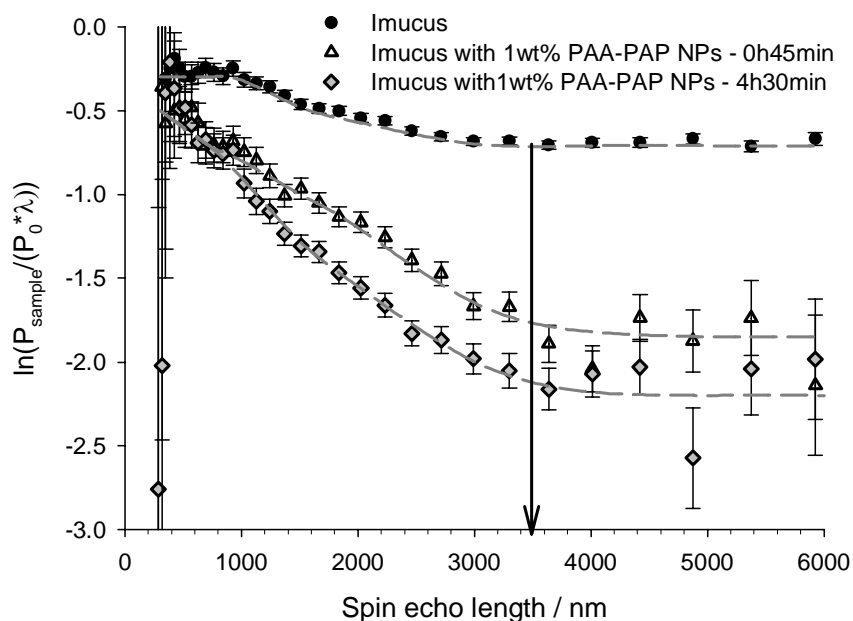
Figure 7. Polarization as a function of spin echo for Imucus and the same in the presence of 1wt% PAA-PAP NPs incubated for 0h45m and 4h30min. The arrow indicates the largest length scale characteristic for the density distribution.

Figure 8. Polarization as a function of spin echo for Imucus and the same in the presence of 1wt% PAA-BRO NPs incubated for 0h10m and 4h30min. The arrow indicates the largest

21
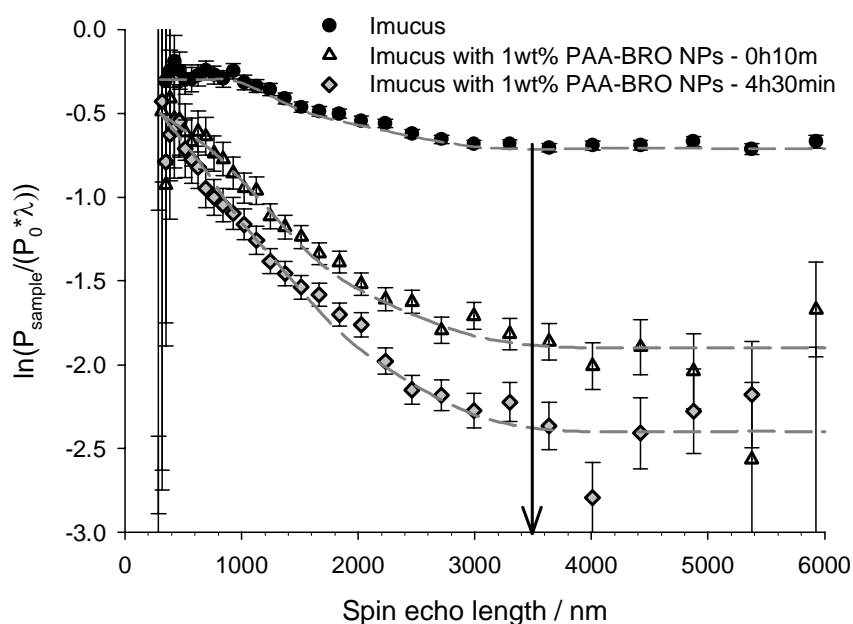
length scale characteristic for the density distribution.

5. DISCUSSION

The formulation of a nanoparticulate carrier exploiting mucolytic agents able to cleave the glycoprotein substructures of mucus is a suitable strategy to improve drug oral bioavailability. Within this research the permeation ability of two NPs systems decorated with mucolytic agents was compared. One system bearing PAP showed enhanced permeation property compared to bare NPs in a preliminary *in vivo* study. The other system bearing BRO should possess at least equal permeation ability, according to rheological tests [7], but being more tolerated by patient, according to human *in vivo* tests [18]. The enzymes were conjugated via carbodiimide chemistry to PAA. The synthesis procedure leads to a high yield and to comparable products in terms of enzyme content. Considering the simple procedure carried out, a scale up seems feasible. The reaction was performed under mild condition that preserved the functionality of both enzymes. However, after conjugation BRO preserved its enzymatic activity to a higher extend compared to PAP. The NPs formulation could be carried out efficiently by ionic gelation method. The enzyme content for both enzyme-decorated NPs was similar and the enzymatic activity maintained.

The cytotoxicity of polymers and particles was assessed by resazurin test. This assay was choose as no need of medium removal after sample incubation is needed. In fact, during the 4 h experiment the cells can detach from the bottom of the wells due to the action of the proteolytic agents leading to false results in case of medium removal. On the one hand, the polymer PAA-BRO resulted to be more toxic than PAA-PAP on Caco-2 cells. On the other hand, both types of particles exhibit low toxicity when incubated at concentrations lower than 0.2 mg/mL.

As particle size and surface charge of the two types of particles were similar, the difference in permeation properties between PAA-PAP NPs and PAA-BRO NPs can be ascribed only to the mucolytic activity of the coupled enzyme and not to the physic-chemical properties of the

23

NPs. The permeation ability of the enzyme decorated NPs through porcine Imucus was first assessed on a mm scale by the rotating tube technique. Exploiting this test it was possible to assess that the conjugation with BRO increased the permeation ability of bare particles to a higher extent compared to PAA-PAP NPs making PAA-BRO NPs a more interesting mucus permeating carrier. **This higher permeation performance of PAA-BRO NPs could be ascribed to the higher stability of BRO upon polymer conjugation resulting in a lower activity loss compared to PAA-PAP NPs.** As control, PAA NPs were analyzed confirming the low permeation feature.

The diffusion of the Imucin was measured by PGSE-NMR. In concentrated biopolymer systems such as mucus, an analysis of the diffusion data is often complex as the observed mobility which may span a wide range of value, is dependent on many factors, including but not limited to the molecular weight, the polydispersity of the diffusing species, the heterogeneity in gel (physical) structure and/or heterogeneity in the mucin (chemical) structure. Therefore, the transport of NPs through such a gel will obviously be dependent on the underlying dynamics of the gel itself (e.g. rheology), superimposed on the effects any interactions between the NPs and the mucin or other components present in the mucus (e,g, protein adsorption to the particle surfaces). Disentangling the relative importance of the underlying gel dynamics and any further retardation of the particles due to specific binding, is essential if one is to isolate the effects of cleavage of the gel, and thus, optimise the delivery strategy.

To this end, the permeation of the NPs through mucus gels, which is a net effect of all interactions, **may be** compared with the NMR determined diffusion of the gel, which is limited to the structure of mucin itself. Therefore, consider first the rather coarse diffusion coefficient ratio derived from the weighted averages of the fast and slow components. When incubated with PAA-PAP and PAA-BRO NPs there is an increase in the rate of diffusion of

the mucin, consistent with the proteolytic cleavage of the mucin strands, leading to polymers of lower molecular weight that will inherently possess a larger diffusion coefficient. This observation confirms that NPs surface decoration with mucolytic enzymes leads to increased permeation. Moreover, it appears that PAA-BRO NPs have the most significant effect on the mucin gel diffusion compared with PAA-PAP NPs. In fact, PAA-BRO NPs action leads to a substantially increased (x10) rate of diffusion of the slow component. These increases are comparable to the increases observed in the permeation study, suggesting a strong correlation between the two facets of the system. However, further work is required to understand the mode of action of the enzyme decorated NPs in order to more fully contrast the relative merits of PAP and BRO, in order to draw out stronger correlations with the permeation enhancement observed in the *in vitro* assay.

Taken together, the two scattering experiments reinforce the insights gained from the diffusion analysis. The bare particles do not lead to any large scale destruction in the structure and thus their mobility through the gel is somewhat limited. The surface decorated particles induce a loss of structure on a long lengthscale but with little effect on the conformation of the constituent polymers. The simple conclusion may be drawn is that the enzymes induce a very localized destruction in cross-linking density, leading to their greater mobility through the mucus associated with a greater mobility of the mucus itself. What is not clear from this data is precisely how the reduction in cross-linking density is achieved but it is known that both enzymes possess a broad specificity. PAP exhibits a preference for hydrophobic amino acid at position P2 especially for Phe and Tyr and for Gly, Met, Cys and Arg at position P1 and does not accept Val at position P1' [32], whereas BRO preferentially cleaves the carbonyl terminal site of lysine, alanine, glycine and tyrosine [33].

6. CONCLUSION

With the aim to design new oral DDSs able to overcome the intestinal mucus barrier PAP and BRO were conjugated to PAA. With these modified polymers NPs could be formulated presenting similar physic-chemical properties in term of particles size, zeta potential and enzyme content. The ability of the NPs in permeating porcine mucus and the changes in the mucus gel layer structure provoke by these systems were evaluated providing an inside from a nanometer to a microns lengthscale. The results obtained from the different technique used showed a strong correlation. In all tests BRO modified NPs exhibit the most significant effect in altering the mucus structure and the higher performance in permeating a fresh mucus layer compared to PAP conjugated NPs. Accordingly, the modification with BRO can further improve the permeability of PAA NPs and, therefore, this system can be exploited as a drug carrier able to transport the therapeutic payload through the mucus barrier and consequently able to improve the bioavailability of orally administered drugs.

REFERENCE

[1] R.A. Cone, Barrier properties of mucus, Advanced drug delivery reviews, 61 (2009) 75-85.
[2] C. Müller, G. Perera, V. König, A. Bernkop-Schnürch, Development and in vivo evaluation of papain-functionalized nanoparticles, European Journal of Pharmaceutics and Biopharmaceutics, 87 (2014) 125–131.
[3] T.-J. Fu, U.R. Abbott, C. Hatzos, Digestibility of Food Allergens and Nonallergenic Proteins in Simulated Gastric Fluid and Simulated Intestinal FluidA Comparative Study, Journal of Agricultural and Food Chemistry, 50 (2002) 7154-7160.
[4] G. Lorkowski, Gastrointestinal absorption and biological activities of serine and cysteine proteases of animal and plant origin: review on absorption of serine and cysteine proteases, International journal of physiology, pathophysiology and pharmacology, 4 (2012) 10-27.
[5] V. Grabovac, T. Schmitz, F. Foger, A. Bernkop-Schnurch, Papain: an effective permeation enhancer for orally administered low molecular weight heparin, Pharm Res, 24 (2007) 1001-1006.
[6] L.P. Hale, Proteolytic activity and immunogenicity of oral bromelain within the gastrointestinal tract of mice, International immunopharmacology, 4 (2004) 255-264.
[7] C. Müller, K. Leithner, S. Hauptstein, F. Hintzen, W. Salvenmoser, A. Bernkop-Schnürch, Preparation and characterization of mucus-penetrating papain/poly(acrylic acid) nanoparticles for oral drug delivery applications, J Nanopart Res, 15 (2012) 1-13.
[8] X. Baur, G. Fruhmann, Allergic reactions, including asthma, to the pineapple protease bromelain following occupational exposure, Clinical allergy, 9 (1979) 443-450.
[9] G. Gailhofer, M. Wilders-Truschnig, J. Smolle, M. Ludvan, Asthma caused by bromelain: an occupational allergy, Clinical allergy, 18 (1988) 445-450.
[10] V. van Kampen, R. Merget, T. Bruning, [Occupational allergies to papain], Pneumologie (Stuttgart, Germany), 59 (2005) 405-410.
[11] A.P. Rosenthal, M.B. Blond, [The enzyme papain in industry and food causes allergic sensitization], Ugeskrift for laeger, 170 (2008) 3127-3129.
[12] E. Nettis, G. Napoli, A. Ferrannini, A. Tursi, IgE-mediated allergy to bromelain, Allergy, 56 (2001) 257-258.
[13] L.E. Mansfield, C.H. Bowers, Systemic reaction to papain in a nonoccupational setting, The Journal of allergy and clinical immunology, 71 (1983) 371-374.
[14] L.E. Mansfield, S. Ting, R.W. Haverly, T.J. Yoo, The incidence and clinical implications of hypersensitivity to papain in an allergic population, confirmed by blinded oral challenge, Annals of allergy, 55 (1985) 541-543.
[15] R. Massimiliano, R. Pietro, S. Paolo, P. Sara, F. Michele, Role of bromelain in the treatment of patients with pityriasis lichenoides chronica, The Journal of dermatological treatment, 18 (2007) 219-222.
[16] N.M. Akhtar, R. Naseer, A.Z. Farooqi, W. Aziz, M. Nazir, Oral enzyme combination versus diclofenac in the treatment of osteoarthritis of the knee--a double-blind prospective randomized study, Clinical rheumatology, 23 (2004) 410-415.
[17] J.M. Braun, B. Schneider, H.J. Beuth, Therapeutic use, efficiency and safety of the proteolytic pineapple enzyme Bromelain-POS in children with acute sinusitis in Germany, In vivo (Athens, Greece), 19 (2005) 417-421.
[18] L. Buttner, N. Achilles, M. Bohm, K. Shah-Hosseini, R. Mosges, Efficacy and tolerability of bromelain in patients with chronic rhinosinusitis--a pilot study, B-ent, 9 (2013) 217-225.
[19] V. Grabovac, D. Guggi, A. Bernkop-Schnürch, Comparison of the mucoadhesive properties of various polymers, Advanced drug delivery reviews, 57 (2005) 1713-1723.
[20] U. Hanefeld, L. Gardossi, E. Magner, Understanding enzyme immobilisation, Chemical Society Reviews, 38 (2009) 453-468.

[21] R.E. Mitchel, I.M. Chaiken, E.L. Smith, The complete amino acid sequence of papain. Additions and corrections, The Journal of biological chemistry, 245 (1970) 3485-3492.

[22] A. Ritonja, A.D. Rowan, D.J. Buttle, N.D. Rawlings, V. Turk, A.J. Barrett, Stem bromelain: Amino acid sequence and implications for weak binding of cystatin, FEBS Letters, 247 (1989) 419-424.

[23] F.M. Ezekiel Amri, PAPAIN, A PLANT ENZYME OF BIOLOGICAL IMPORTANCE: A REVIEW, American Journal of Biochemistry and Biotechnology, 8 (2012) 99-104.

[24] T. Murachi, [39] Bromelain enzymes, in: L. Laszlo (Ed.) Methods in Enzymology, Academic Press, 1976, pp. 475-485.

[25] S. Yodoya, T. Takagi, M. Kurotani, T. Hayashi, M. Furuta, M. Oka, T. Hayashi, Immobilization of bromelain onto porous copoly(γ-methyl-l-glutamate/l-leucine) beads, European Polymer Journal, 39 (2003) 173-180.

[26] C. Taylor, A. Allen, P.W. Dettmar, J.P. Pearson, Two rheologically different gastric mucus secretions with different putative functions, Biochimica et biophysica acta, 1674 (2004) 131-138.

[27] S.C. Pereira de Sousa I., Schmutzler M., Wilcox M.D., Veldhuis G.J., Pearson J.P., Huck C.W., Salvenmoser W., Bernkop-Schnürch A., Mucus permeating carriers: formulation and characterization of highly densely charged nanoparticles, European Journal of Pharmaceutics and Biopharmaceutics, (2014).

[28] P.T. Callaghan, Principles of Nuclear Magnetic Resonance Microscopy, Oxford University Press, Oxford, 1991.

[29] P. Stilbs, K. Paulsen, P.C. Griffiths, Global Least-Squares Analysis of Large, Correlated Spectral Data Sets: Application to Component-Resolved FT-PGSE NMR Spectroscopy, The Journal of Physical Chemistry, 100 (1996) 8180-8189.

[30] C.M. Sorensen, A. Chakrabarti, The sol to gel transition in irreversible particulate systems, Soft Matter, 7 (2011) 2284-2296.

[31] H. Wu, J. Xie, M. Lattuada, J. Kohlbrecher, M. Morbidelli, Effect of Primary Particle Size and Salt Concentration on the Structure of Colloidal Gels†, The Journal of Physical Chemistry C, 115 (2010) 931-936.

[32] A. Davy, S.L. MB, I. Svendsen, V. Cameron-Mills, D.J. Simpson, Prediction of protein cleavage sites by the barley cysteine endoproteases EP-A and EP-B based on the kinetics of synthetic peptide hydrolysis, Plant physiology, 122 (2000) 137-146.

[33] J.F. Kennedy, C.A. White, Industrial enzymology: The application of enzymes in industry. Edited by Tony Godfrey and Jon Reichelt, Macmillan, The Nature Press, London, 1983. Pp x + 582, Price £40.00. ISBN 0943818001, British Polymer Journal, 16 (1984) 60-60.

CAPTIONS:

Table 1. Characteristics of the synthetized polymers. Results are the mean of four different synthesis of each polymer (± standard deviation).

Table 2. Characteristics of the tested nanoparticles. Results are the mean of four different formulations per each sample (± standard deviation).

Table 3. Absolute and relative diffusion coefficients for Imucin in the presence of the three nanoparticles; PAA NPs, PAA-PAP NPs and PAA-BRO NPs.

Figure 1. Schematic representation of the rotating tube technique.

Figure 2. Cytotoxicity of PAA-PAP (white bars), PAA-PAP NPs (dotted bars), PAA-BRO (gray bars) and PAA-BRO NPs (striped bars) determined by resazurin assay after 4 h incubation with Caco-2 cells. Values are the means of three experiments (± standard deviation).

Figure 3. Permeation studies of PAA NPs (black bars), PAA-PAP NPs (dotted bars) and PAA-BRO NPs (gray bars), in porcine Imucus. Particles suspended in SIF pH 6.8 were incubated for 4 h at 37°C. * $p<0.05$ vs PAA NPs, ** $p<0.05$ vs PAA-PAP NPs. Values are the means of six experiments (± standard deviation).

Figure 4. Raw PGSE-NMR data from which the diffusion coefficient of the Imucin and related components were extracted.

Figure 5. Scattering intensity I(Q) as a function of wavevector Q for Imucus and the same in the presence of 1wt% PAA-PAP NPs and the equivalent amount of free enzyme.

Figure 6. Scattering intensity I(Q) as a function of wavevector Q for Imucus and the same in the presence of 1wt% PAA-BRO NPs and the equivalent amount of free enzyme.

Figure 7. Polarization as a function of spin echo for Imucus and the same in the presence of 1wt% PAA-PAP NPs incubated for 0h45m and 4h30min. The arrow indicates the largest

length scale characteristic for the density distribution.

Figure 8. Polarization as a function of spin echo for Imucus and the same in the presence of 1wt% PAA-BRO NPs incubated for 0h10m and 4h30min. The arrow indicates the largest length scale characteristic for the density distribution.

Poly(acrylic) acid

P Papain

B Bromelain

CaCl₂

CaCl₂

CaCl₂

Intestinal mucus
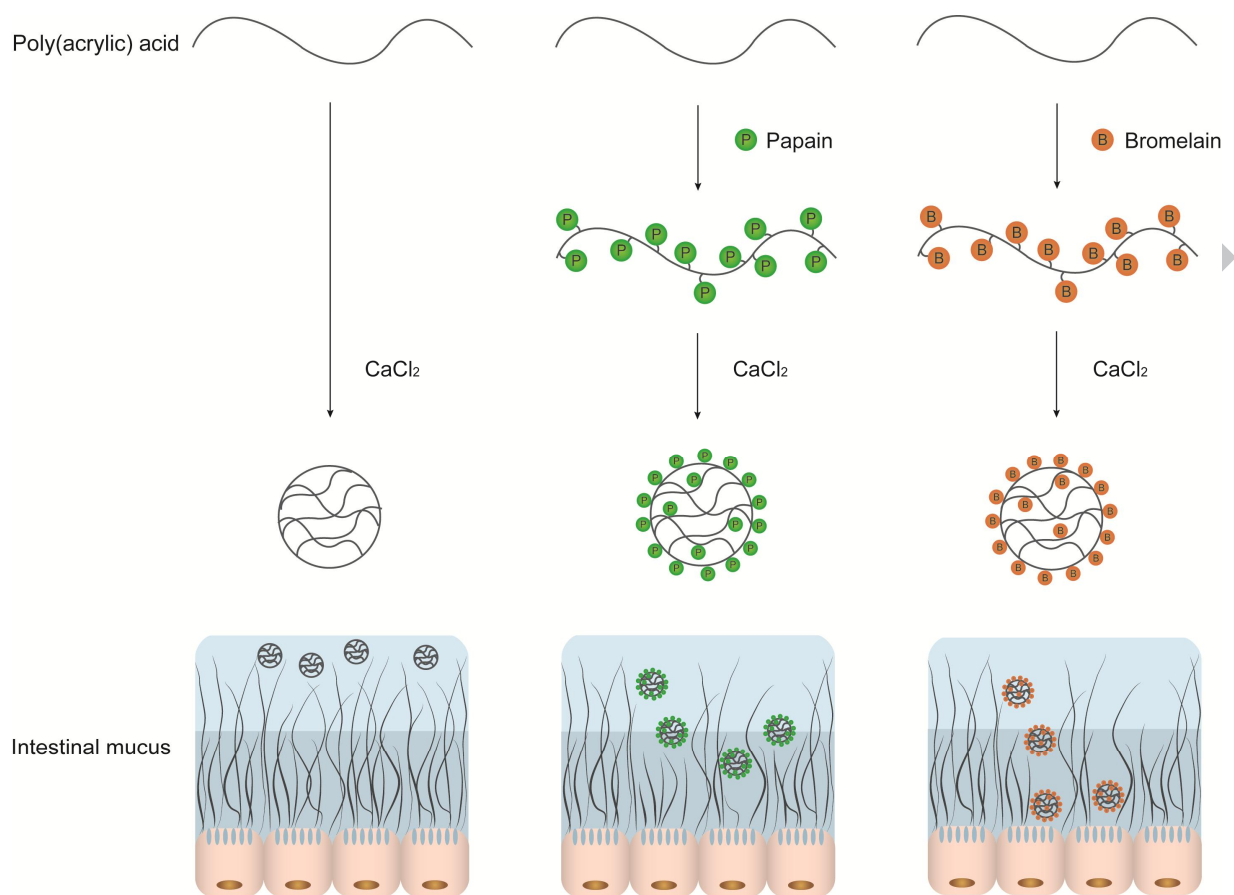
- Nanoparticles were formulated with papain and bromelain modified poly(acrylic acid)
- Inside from a nm to a μm lengthscale of particles mucus permeation ability is given
- Particles bearing bromelain show higher permeation ability then papain particles
- Bromelain particles exhibit the most relevant effect in altering mucus structure
- Bromelain decorated particles can be exploited as oral drug delivery system